

Mechanical Properties of Externally Invisible Furniture Joints Made of Wood-Based Composites

Jerzy Smardzewski,^{a,*} Błażej Rzepa,^a and Halil Kılıç^b

The aim of this investigation was to design and determine the mechanical properties of innovative, externally invisible, 3D-printed cabinet furniture joints that can be assembled without the use of tools. The cognitive objective of the study was to ascertain the stiffness and strength of designed joints that differed in the number and length of fasteners, as well as in the kind of connected panel materials. During the tests, a digital image analysis method was used for verifying analytical calculations. The finite element method was used for determining the mechanical properties of joints. Results showed that the joint designed with a dual-conical fastener was characterized by high stiffness and strength. The stiffness and strength of the joint depended on the number and length of fasteners. The low level of stress in the panel elements guaranteed durable, safe utilization of cabinet furniture made of medium density fiberboard and particleboard. In conclusion, ease of assembly and disassembly of joints without tools, external invisibility, good aesthetics, high resistance, and stiffness ensure a high potential for 3D-printed cabinet furniture joints in industry and trade.

Keywords: Furniture; Invisible joint; easy-to-assemble; Design; Numerical analysis

Contact information: a: Department of Furniture Design, Faculty of Wood Technology, Poznan University of Life Sciences, Poznan, Poland; b: Department of Woodworking Industrial Engineering, Faculty of Technology, Muğla Sıtkı Koçman University, Muğla, Turkey;

*Corresponding author: jsmardzewski@up.poznan.pl

INTRODUCTION

There have been many studies that have aimed to determine the mechanical properties of furniture corner joints. These studies have analyzed the relationship between joint types, joint components (such as number of joints), adhesion, adhesive, screw type, and wood or wood-based panels. Joints are the weakest parts of furniture; thus, their design is very important. Even though furniture components have enough strength to carry the loads that the furniture bears, joint failure can negatively affect the whole furniture structure. In this respect, it is vitally important to make safe scientific designs to carry the loads for each component of the furniture construction (Eckelman 2003; Smardzewski 2015b).

Only a couple of published papers have considered the strength of ready-to-assemble joints. Derikvand and Eckelman (2015) investigated the strength of the glued joint with butterfly dovetail keys. Joints constructed with two dowels had slightly greater bending moment capacity than splined miter joints and a substantially greater capacity than joints constructed with a single dowel, glued, or unglued butterfly keys, or glued or unglued H-shaped keys. Altun *et al.* (2010) studied the influence of the type of adhesive in the miter corner joints with dovetail fitting on bending moment capacity under diagonal tensile and compression loading were considered, and the joints without adhesive were compared. The

highest bending moment capacity under diagonal loading was obtained in the specimens bonded with adhesive. Efe and Kasal (2000) compared the tensile strength properties of stable and portable corner joints with case construction prepared from particleboard (PB) and medium density fiberboard (MDF). Kasal (2008) studied the effect of the number of screws and screw size on the moment capacity of furniture corner joints. He tested specimens under static compression and tension loads, and his results showed that the maximum moment capacity is obtained by MDF specimens when the number of screws in the joints is four. In both compression and tension tests, MDF corner joints were stronger than PB corner joints. Rajak and Eckelman (1996) indicated that the bending strength of corner joints was directly proportional to the number of fasteners. The bending strength of a two-fastener joint was twice as strong as that of a single-fastener joint. Furthermore, the authors suggested that the most appropriate screw spacing was 102 mm for a board 19 mm in thickness. Zhang *et al.* (2005) investigated the effects of screw size, loading, material type, panel surface condition, and gluing on the moment resistances of three-screw L-type corner joints with tension and compression tests. Results showed that surfacing PB with synthetic resin and assembling joints with glue applied to the contact surfaces of the face and butt members obtained noticeably better moment resistances than joints constructed of only PB.

Thus far, most investigations on the bending moment capacity of joints have been conducted to observe the gross values of the bending resistance of test specimens (Zhang and Eckelman 1993; Ching and Yiren 1994; Vassiliou and Barboutis 2005; Kasal *et al.* 2006; Atar *et al.* 2009, 2010). The bending moment resistances of corner joints for cases constructed of 32-mm-thick laminated PB and MDF, under compression and tension loads, have been investigated (Tankut 2005). Örs and Efe (1998) studied the mechanical properties of furniture fasteners in frame-type furniture and concluded that joints constructed with minifix and multifix fasteners are better than traditional glue-type joints. Tankut and Tankut (2008) studied the strength of corner joints in case-type furniture construction under the effects of fastener, glue, and composite material type. Based on previous studies, it can be seen that there are not enough studies about cabinet furniture corner joints that do not require the use of adhesive, screws, or tools for assembly. No effort has been made to analyze 3D-printed furniture corner joints.

The aim of this investigation was to design innovative, externally invisible, cabinet furniture joints that can be assembled without the use of tools. The cognitive objective of the study was to ascertain the stiffness and strength of designed joints that differed in the number and length of fasteners, as well as in the kind of connected panel materials. The practical goal of the experiments was to demonstrate that joints designed for assembling furniture without tools are useful and have the potential to be failsafe.

EXPERIMENTAL

Design of a Fastener and Furniture Joints

When designing the novel joint, it was assumed that it ought to consist of a single externally-invisible fastener; allow furniture assembly and disassembly without the assistance of tools; be stiff and strong; and be technically feasible, possibly cheap, and able to connect varying materials. Employing ingenious and inventive methods, a construction solution was developed (Smardzewski 2015a), protected by a P412167 patent application. It consisted of a fastener, manufactured from poly-acrylonitril-butadiene-styrene (ABS)

using Flashfarge 3D Sygnis (China) printer technology, whose shape and dimensions are presented in Fig. 1 including side and front views. The two lengths of the fasteners measured between axis semicircles that were adopted for experiments were 4 mm and 30 mm. Appropriate slots were made in the elements of type L angle joints (Fig. 2).

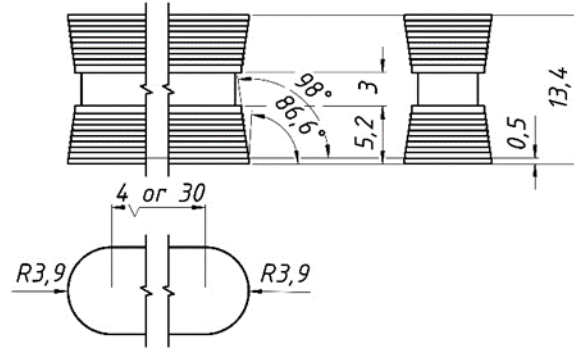


Fig. 1. Fasteners 4 mm and 30 mm long

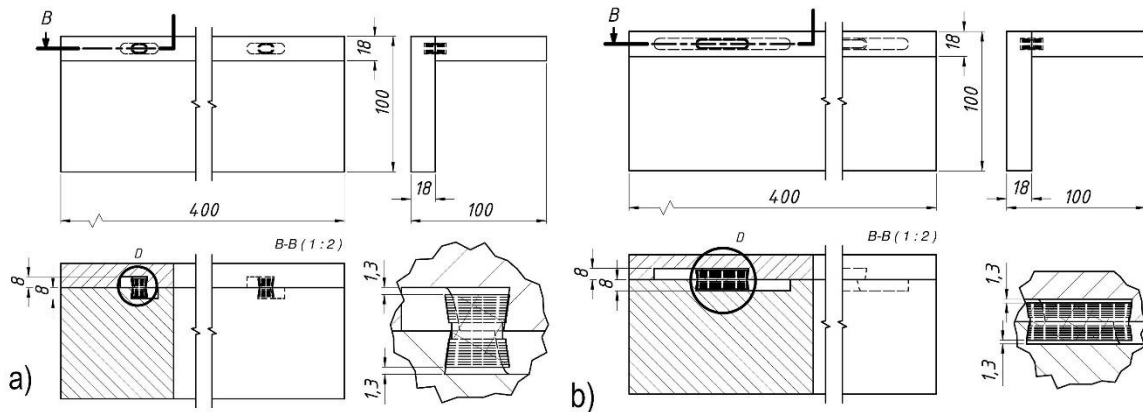


Fig. 2. Joints with fasteners of lengths: a) 4 mm, b) 30 mm

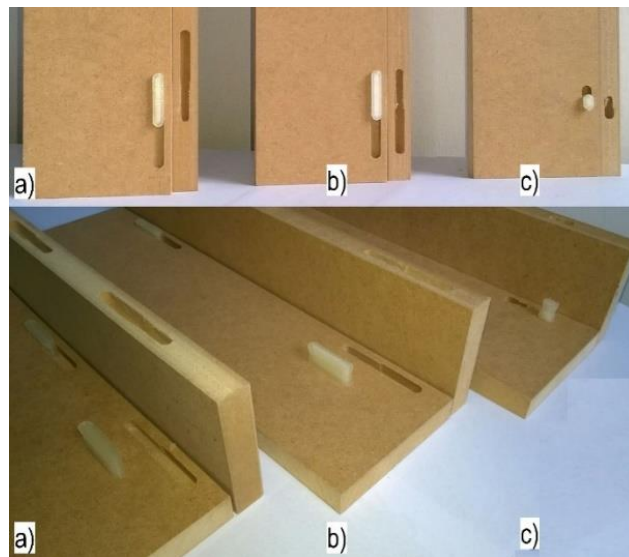


Fig. 3. MDF joints: a) three 30-mm-long fasteners, b) two 30-mm-long fasteners, c) two 4-mm-long fasteners

The shape of these slots made it possible to freely insert the fastener into one element, placing the slot of the second element onto the fastener and, then, sliding the two elements in the direction perpendicular to that of the fastener. The reciprocal shift of the elements triggered internal forces on contact surfaces and a growing pressure at the contact of the two elements. The disassembly of the joints occurred in reverse order. Fiberboard and MDF panels 18 mm thick were employed to prepare experimental joints. For each panel type, respectively, joints with two or three fasteners were applied. Distances between fasteners, depths of slots, and method of fastener mounting are presented in Fig. 2 including side and front views. Figure 3 shows the shape of fasteners as well as slots made in the elements from MDF panels.

Table 1. Type of Joints

Code of joint	Type of material	Number of connectors	Length of connectors (mm)
M2-4	MDF	2	4
M2-30		2	30
M3-30		3	30
P2-4	PB	2	4
P2-30		2	30
P3-30		3	30

Table 2. Physico-Mechanical Properties of Materials

Properties	Type of material					
	MDF		PB		ABS	
	Average	SD	Average	SD	Average	SD
E (MPa)	3778	192	3297	161	1118	60.3
G (MPa)	1453	-	1268	-	600	-
MOR (MPa)	26.6	1.4	14.5	0.7	40.0	5.34
ν	0.30	-	0.30	-	0.41	-
ρ (kg/m ³)	703	5.8	615	12.9	1290	95.5
$R_{0,05}$ (MPa)	5.22	0.63	1.87	0.21	3.82	0.42
$R_{0,2}$ (MPa)	26.60	2.13	14.5	1.42	40.0	4.96
MC (%)	5.0	0.3	6.2	0.3	-	-

Table 1 illustrates variants of joints used in the study. For each type of joints, 10 samples were used. For the investigation a total of 120 samples and 280 connectors was prepared. Table 2 presents the mechanical properties of materials from which fasteners and joint elements were prepared. Bending tests, for determining modulus of elasticity and modulus of rupture of MDF and PB, were conducted in accordance with the requirements of the EN 310 standard (1994). The Poisson's ratio for both materials was assumed to be 0.3. On the basis of the equation $G = E / (2(1 + \nu))$, values of shear modulus were calculated. Density and moisture content of wood based materials were determined according EN 323 and EN 322 standards (1993). Their elastic $R_{0,05}$ and plastic $R_{0,2}$ limits were determined according to standard NT BUILD 316 (1986). The mechanical properties of ABS were collected on the basis of the technological requirements defined by the manufacturer (<http://www.materialise.pl>).

Stiffness of Joints

The mechanical properties of experimental joints were determined on the basis of tensile (Fig. 4a) and compression (Fig. 4b) tests. Experiments were carried out using a

numerically controlled test machine (Zwick 1445, Germany) recording force P with 0.01 N accuracy, and displacement DP with the accuracy of 0.01 mm. The speed of loading was 10 mm/min. Procedures were terminated when the loading had decreased by 20 N or when the displacement along the action of force P exceeded the value of $DP = 10$ mm. In addition, in each test, the authors determined the value change of the angle Df between arms of the joint. For this purpose, analytical calculations were applied (Fig. 5) and verified by measurements taken using digital image analysis (Smardzewski *et al.* 2015). The above measurements were performed with the assistance of a Basler A102k (Germany) monochromatic camera, frame grabber card NI PXIe-1435 (Germany), and IMAQ Vision software from National Instruments (Fig. 6). The strength of a joint was expressed as the highest value of the bending moment that caused construction damage.

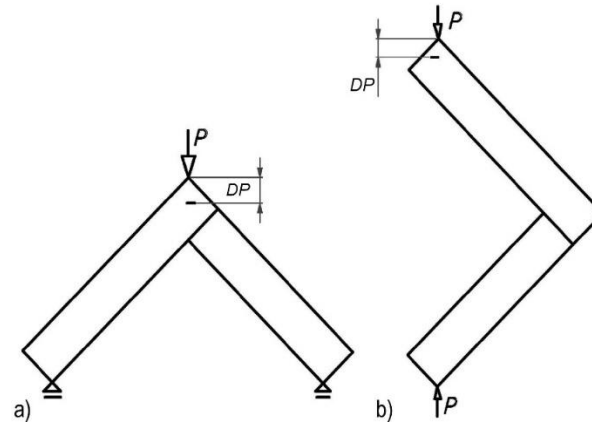


Fig. 4. Method of joint loading: a) tensile, b) compression

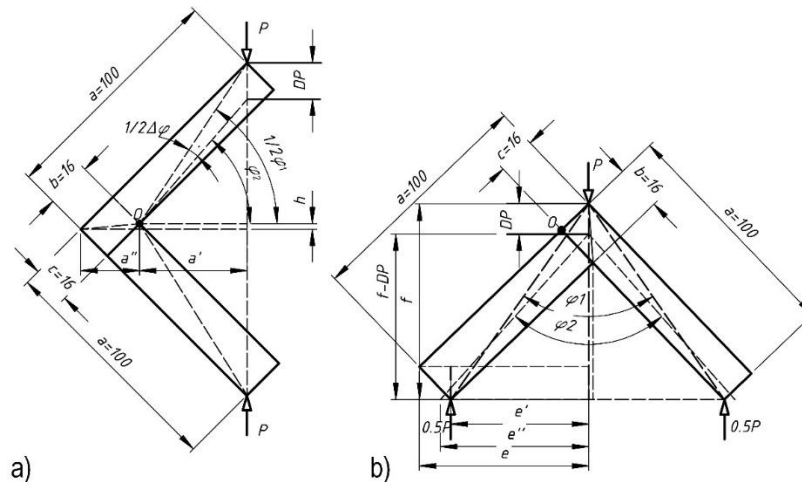


Fig. 5. Measurements necessary to calculate stiffness coefficient K : a) tensile, b) compression (Smardzewski *et al.* 2015)

Analytically, stiffness of a joint was determined on the basis of the analysis of the joint geometry change during loading with force P (Fig. 5). In the compression test of the joint (Fig. 5a), its stiffness was determined using the following equations,

$$K = \frac{M}{\Delta\varphi} = \frac{Pa'}{\Delta\varphi} \text{ [Nm/rad]} \quad (1)$$

where:

$$\Delta\varphi = \frac{\pi}{90}(\varphi_1 - \varphi_2) \quad (2)$$

$$a' = \frac{\sqrt{2}}{2}a - a'' \quad (3)$$

$$a'' = \sqrt{b^2 + c^2 - h^2} \quad (4)$$

$$h = \frac{\sqrt{2}}{2}(b - c) \quad (5)$$

$$\varphi_1 = \text{atg}\left(\frac{\frac{\sqrt{2}}{2}a - h}{a'}\right) \quad (6)$$

$$\varphi_2 = a \sin\left(\frac{\frac{\sqrt{2}}{2}a - h - DP_{0.4P_{\max}}}{\sqrt{c^2 + (a-b)^2}}\right) \quad (7)$$

and $DP_{0.4P_{\max}} = 0.4 \times DP_{\max}$

The stiffness of the joint subjected to the tensile test (Fig. 5b) was calculated from the following equation:

$$K = \frac{M}{\Delta\varphi} = \frac{Pe'}{\Delta\varphi} \text{ [Nm/rad]} \quad (8)$$

where:

$$\Delta\varphi = \frac{\pi}{90}(\varphi_2 - \varphi_1) \quad (9)$$

$$e' = \frac{\sqrt{2}}{2}(a - b) \quad (10)$$

$$0.5\varphi_1 = \text{atg}\left(\frac{e'}{f}\right) \quad (11)$$

$$0.5\varphi_2 = \text{atg}\left(\frac{e''}{f - DP_{0.4P_{\max}}}\right) \quad (12)$$

$$f = e + \frac{\sqrt{2}}{2}b \quad (13)$$

$$e = \frac{\sqrt{2}}{2}a \quad (14)$$

$$e'' = \sqrt{e'^2 + f^2 - (f - DP_{0.4P_{\max}})^2} \quad (15)$$

The correctness of the above model was verified by optically measuring deflections of arms and displacements of selected points (Fig. 6). Using reference photographs taken following the initial loading of joints with the force of 10 N, the following values were determined on non-deformed samples: length of the $\overline{12'}$ segment and the angle $\angle 345'$ (Figs. 6a, 6c). For the maximum loading, additional pictures were taken on deformed samples. On this basis, the following values were determined: length of the $\overline{12''}$ segment as well as the angle $\angle 345''$ (Figs. 6b, 6d). The positions of the camera, light sources, and their power (2 x 60 W) were not changed when taking the photos. $DP = \overline{12'} - \overline{12''}$ displacements and $\Delta f = \angle 345' - \angle 345''$ deformations were calculated on

the basis of differences between measurements established both from reference pictures and from final photographs.

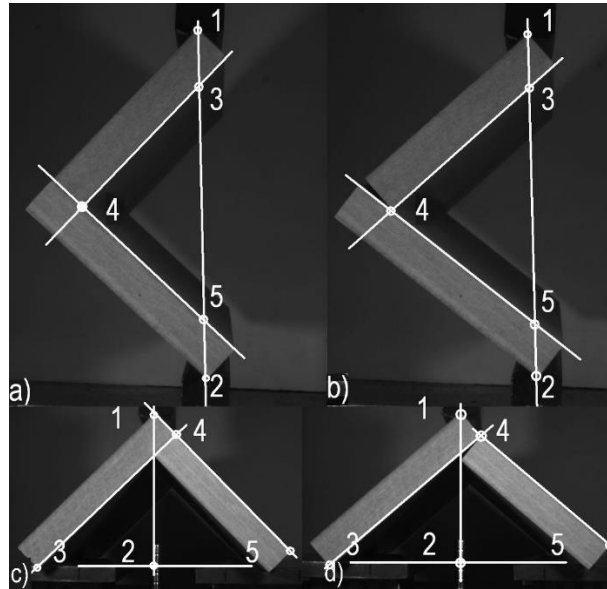


Fig. 6. Displacement measurement using the method of digital image analysis: a) and b) compression; c) and d) tensile

Strength of Joints

Strength of joints was ascertained by comparing the maximal bending moments that cause their failure. In the case of joints subjected to compression, the $M = Pa'$ formula was applied. For joints subjected to tensile stress, the $M = Pe'$ formula was employed. The authors determined joint strength by using numerical calculations of the finite element method. The quality of the strength calculations obtained was verified by comparing displacement results DP determined numerically and experimentally. The compatibility of the examined displacements was guaranteed by the quality of the elaborated numerical model and the results of strength calculations.

Before proceeding to numerical calculations, the authors analyzed the statics of the system formed by the fastener pressing on walls of the slot (Fig. 7a). The force that guaranteed appropriate stiffness of the joint was the assembly force F_A caused by the reciprocal movement of joint elements. The perpendicular movement of the fastener in slots to the wide surfaces of the elements exerted pressure with force N on surfaces of three side walls. In this particular case, those surfaces included two flat A_1 surfaces and one A_2 surface that constituted a side surface of a truncated cone. The equilibrium equation for this state of loads can be presented as follows,

$$\sum X = 0 = 3T \cos \alpha + 3N \sin \alpha - F_A \quad (16)$$

where T is the force of friction and α is the inclination angle of side walls of the fastener when,

$$T = \mu N = \tan \alpha N \quad (17)$$

where μ is the friction coefficient between surfaces. Hence:

$$F_A = 3N(\tan \alpha \cos \alpha + \sin \alpha) \quad (18)$$

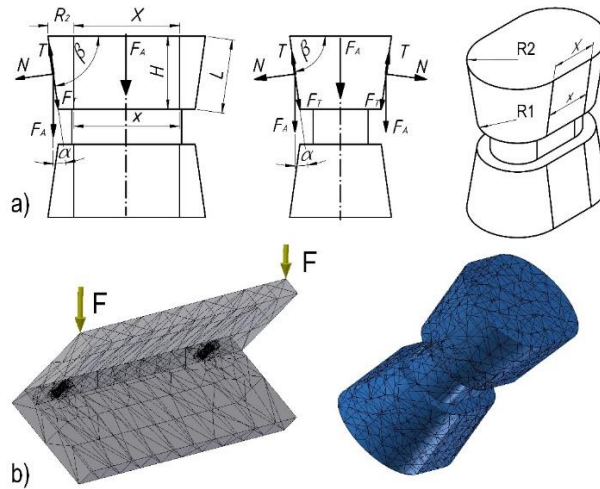


Fig. 7. Joint model: a) analytical, b) FEM

Because the value of normal force N depends on the size of flat surfaces A_1 , the conical surface A_2 and normal stress σ ,

$$N = \sigma(2A_1 + A_2) \quad (19)$$

$$A_1 = 0.5(X + x)H \quad (20)$$

$$A_2 = \pi(R_2 + R_1)L \quad (21)$$

$$L = (H^2 + (R_2 - R_1)^2)^{0.5} \quad (22)$$

the value of the assembly force necessary to obtain a stiff and resistant joint can be expressed by the following equation,

$$F_A = 3k_{\text{MDF}}^c \left((X + x)H + \pi(R_2 + R_1)(H^2 + (R_2 - R_1)^2)^{0.5} \right) (\tan \alpha \cos \alpha + \sin \alpha) \quad (23)$$

where k_{MDF}^c is the compression strength of the material (*e.g.*, MDF).

It is evident from this equation that the value of the assembly force depends on the shape and dimensions of the fastener, and this, in turn, affects joint stiffness. Bearing this in mind, a numerical model was prepared for two reference joints, M2-4 and M3-30, manufactured from MDF panels and subjected to compression with force P corresponding to the linear elasticity limit $R_{0.05}$. It was assumed that positive verification of these models would also allow their application in the case of the remaining joints.

Figure 7b presents a representation of a lattice model of the M2-4 joint. Calculations were performed in the Autodesk Simulation Mechanical 2015 (USA) software employing six- and eight-node isotropic brick-type finite elements. Contact areas between fasteners and slots were defined to correspond to their respective counterparts in the physical model. The adopted elastic properties of materials were those obtained in our own experiments and are presented in Table 2. Because the elastic properties of the employed materials referred only to the range of linear elasticity $R_{0.05}$, numerical calculations were also carried out only for this range. That is why load P for the selected joints was assumed on the basis of Table 3 for the $R_{0.05}$ limit, and numerically calculated displacements were confronted with respective displacements for the $R_{0.05}$ limit.

RESULTS AND DISCUSSION

Stiffness of Joints

A dominant evaluation determinant of cabinet furniture joint quality is their stiffness, which is most frequently expressed as the maximal bending moment as a function of displacement or angle of non-dilatational strain. Figure 8 illustrates the variability of the stiffness coefficient K of the examined joints depending on the angle change of the non-dilatational strain Df .

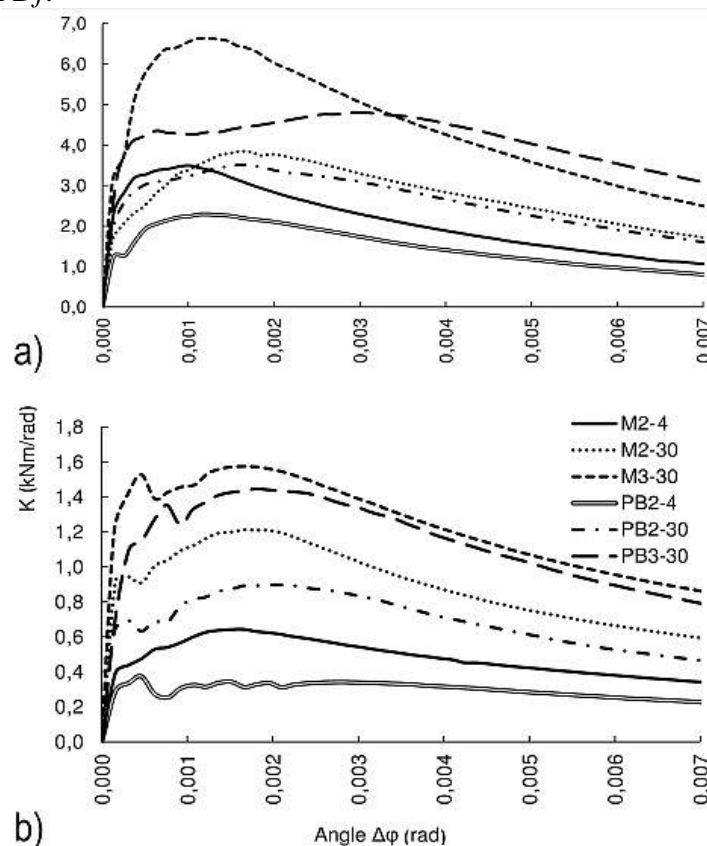


Fig. 8. Dependence of the stiffness coefficient K on the deformation angle Df : a) tensile, b) compression

From this figure, the first important regularity, confirmed by many publications, becomes apparent—namely, that the stiffness of joints subjected to tensile stress (Fig. 8a) was three to five times greater when compared with the stiffness of joints subjected to compression (Fig. 8b) (Atar and Özçi fçi 2008; Atar *et al.* 2009; Altinok *et al.* 2009; Altun *et al.* 2010; Tankut and Tankut 2010; Yerlikaya 2012; Yerlikaya and Aktas 2012; Smardzewski *et al.* 2015). In the range of deformations up to 0.0005 rad, joint stiffness increased almost linearly. Maximum values became visible at deformations of 0.001 rad and 0.002 rad during joint tensile and compression stresses, respectively. Once the above deformations were exceeded, joint stiffness decreased. This indicated that there was progressive permanent destruction of the material structure from which the elements of the joints were manufactured. It can also be seen in Fig. 8 that relationships between individual types of joints were similar in both the tensile test and compression test. From the point of view of quality, M3-30 joints made from MDF panels employing fasteners 30 mm long were characterized by the highest stiffness. Similar P3-30 joints made from fiberboard

panels exhibited slightly higher stiffness. Lower stiffness was determined in joints with two 30-mm-long fasteners mounted in MDF and fiberboard panels (M2-30, P2-30). The lowest stiffness was determined in M2-4 and P2-4 joints consisting of two short fasteners. It is therefore possible to generalize that the length and number of fasteners determined the stiffness of the examined furniture joints. Similar conclusions have been drawn by other researchers who investigated similar or different joints (Liu and Eckelman 1998; Vassiliou and Barboutis 2005; Zhang *et al.* 2005; Kasal *et al.* 2006, 2008a,b; Altinok *et al.* 2009; Yerlikaya 2012; Malkoçoğlu *et al.* 2013).

Furthermore, quantitative differences in stiffness between joints manufactured from MDF and fiberboard panels for some joints were negligible. Details of these differences are collated in Fig. 9, which presents the maximum values of the stiffness coefficient K (Nm/rad) and bending moment M (Nm).

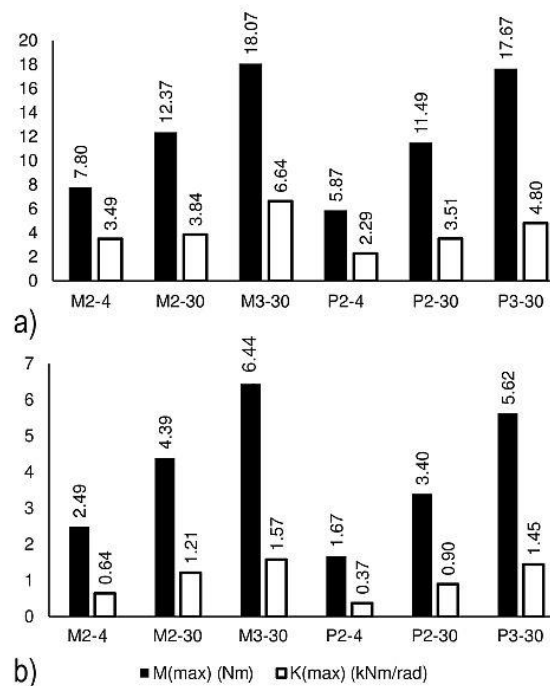


Fig. 9. Maximum stiffness coefficients K and maximum bending moments M : a) tensile, b) compression

It is evident from Fig. 9a that, in the case of stretched M3-30 joints, the stiffness coefficient K was 2.2% higher in comparison with the stiffness coefficient of P3-30 joints. For consecutive joints subjected to tensile stress, M2-30 and P2-30, as well as M2-4 and P2-4, the above differences were +7.7% and 32.8%, respectively. In the case of joints subjected to compression (Fig. 9b), for the compared pairs—M3-30, P3-30; M2-30, P2-30; M2-4, P2-4—the determined differences amounted to 14.5%, 29.1%, and 49.1%, respectively. The above collation makes it possible to draw a conclusion that, in the case of the three 30-mm-long fasteners, the type of material employed only slightly affected joint stiffness. For the remaining solutions, the type of material exerted a strong, negative influence on the stiffness coefficient K . In addition, its value also decreased as a result of declining number and length of fasteners. Comparing values of the stiffness coefficient K within the range of one kind of material and tensile load, differences between M3-30 and, respectively, M3-30 and M2-30 amounted to 46.1% and 58.6%.

Strength of Joints

Trends similar to those recorded in the case of the stiffness coefficient were also observed with respect to joint strength (Fig. 9). The obtained results are corroborated by studies conducted by such researchers as Nicholls and Crisan (2002), Tankut (2005), Kasal (2008), Kureli and Altinok (2011), Maleki *et al.* (2012), and İmirzi and Efe (2013). In the analyzed case, the highest strength was recorded for M3-30 joints subjected to tensile stress, for which $M = 6.64$ Nm, whereas M2-30 and M2-4 joints exhibited lower strength by 72.9% and 90.2%, respectively. On the other hand, the strength of P3-30 joints made from a fiberboard panel was $M = 4.80$ Nm, 38.4% lower than the strength of the M3-30 joint. Also, the strength of P2-30 and P2-4 joints was, respectively, 9.4% and 52.4% lower in comparison with the strength of MDF joints. It can also be seen in Fig. 9b that similar relationships occurred between joints subjected to compression. Respective joint strength changes as a function of angle changes of the non-dilatational strain Df are presented in Fig. 10.

It is clear from Fig. 10 that, together with the increase in the joint arm deflection, their strength increased. This was directly connected to the pressure of the wedge-shaped surfaces of the fasteners on the slot surface. Together with the increase of force F_A (Eq. 23) resulting from bending the arms of the joints, the contact area between the fastener and the slot increased, accompanied by increased surface pressures to the limit of material plasticity $R_{0.2}$ (Table 2). Additionally, the strength of joints reached asymptotic values for deformations $Df > 0.004$ rad. Relationships presented in Figs. 9 and 10 unequivocally corroborate the regularity that emerged during the stiffness analysis of joints. Increased number and length of fasteners enhanced the compression and tensile strength of joints. Moreover, MDF joints demonstrated greater strength than joints made of fiberboard panels.

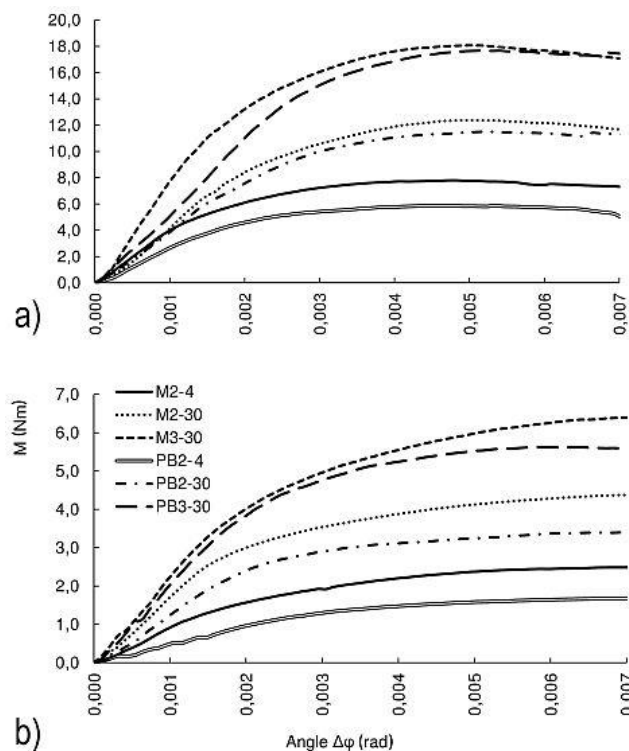


Fig. 10. Dependence of the bending moment M on the deformation angle Df : a) tensile, b) compression

Table 3 collates additional information regarding stiffness and strength of the examined joints. This table presents values of forces P as well as values of displacements DP corresponding to these forces for the limit of linear elasticity $R_{0.05}$ as well as plasticity limit $R_{0.2}$ (*i.e.*, at sample failure). From among data for M2-4 and M3-30 joints subjected to compression, the authors selected corresponding loads to the limit of linear elasticity $R_{0.05}$, *i.e.*, 30.5 N and 55.6 N and linear displacements of 1.79 mm and 1.19 mm corresponding to these forces. The selected concentrated forces were applied in the above-discussed numerical models, and displacements obtained as a result of these calculations were compared with corresponding displacements selected from Table 3.

Table 3. Force and Displacement to the limits of $R_{0.05}$ and $R_{0.2}$

Type of material	Limit	Force or displacement	Compression / type of joint			Tensile / type of joint		
			M2-4	M2-30	M3-30	P2-4	P2-30	P3-30
MDF	$R_{0.2}$	Force (N)	51.8	91.3	134.0	131.3	208.2	303.2
		Displacement (mm)	7.65	7.91	8.80	4.82	4.92	4.99
	$R_{0.05}$	Force (N)	30.5	41.7	55.6	76.6	85.6	148.5
		Displacement (mm)	1.79	1.16	1.19	1.19	1.17	1.15
PB	$R_{0.2}$	Force (N)	34.8	70.7	117.0	98.9	193.5	297.4
		Displacement (mm)	7.55	7.04	6.39	4.59	5.22	5.41
	$R_{0.05}$	Force (N)	12.3	33.7	49.8	52.7	77.1	99.1
		Displacement (mm)	1.27	1.28	1.17	1.19	1.15	1.14

Figure 11a and 11b show displacements DP of M2-4 and M3-30 joints. The comparison of the obtained values, 1.792 mm and 1.05 mm, with displacements determined in the laboratory, 1.79 mm and 1.19 mm, revealed very slight differences ranging from 0.1% to 13.3%. These small differences mean that the numerical model was elaborated correctly, and real elastic properties of the material applied in the elements of experimental joints corresponded to those from Table 2. Similar assumptions were adopted in studies dealing with comparable problems (İmirzi and Efe 2013; Smardzewski *et al.* 2015).

On the other hand, Figs. 11c and 11d show von Mises reduced stresses in plastic fasteners. For the joint with two fasteners 4 mm long, stresses in the fastener reached 58.2% of ABS strength. In the case of the joint with three fasteners 30 mm long, these stresses were not greater than 11.9% of this strength. However, the most important stresses were those generated by fasteners in panel elements. Figures 11e and 11f present the form of von Mises reduced stresses on surfaces of the slot. It is evident that, for the M2-4 joint in the range of $R_{0.05}$, maximal stresses did not exceed 5.6 MPa. This result corresponded to 21.1% of the MDF panel strength. In the case of the M3-30 joint, maximum stresses in the slot did not exceed 2.93 MPa, which constituted 11.0% of the material strength. In addition, results of numerical calculations showed that within the range of linear elasticity of $R_{0.05}$, joints exhibited considerable reserves of strength. That is why, as demonstrated by laboratory experiments, their asymptotic strength increased and, within the set interval of deformations, remained on a constant level (Fig. 10).

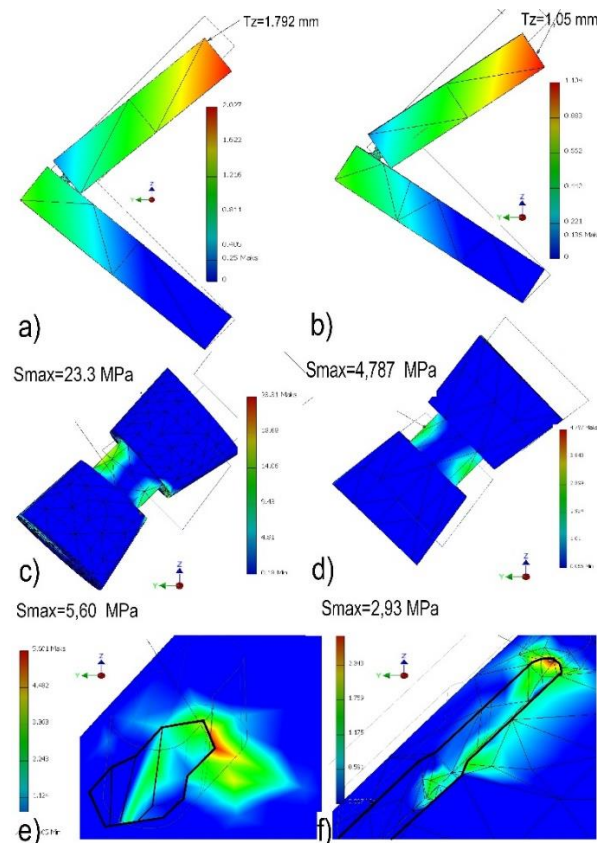


Fig. 11. Results of numerical calculations of M2-4 and M3-30 joints subjected to compression, respectively: a) and b) DP displacements; c) and d) maximum von Mises stresses in the fastener; e) and f) maximum von Mises stresses in the in the slot

In this point of work, it would be worthwhile to compare the advantages and disadvantages of the new connectors over dovetail key joining technique. Derikvand and Eckelman (2015), Altun *et al.* (2010) suggested that the use of dovetail keys is very easy to use. It could be suggested that is a lot easier than the proposed method. For example, the slots for dovetail keys can be routed by using only one specific router bit, whereas routing the slots for the new connectors requires two router bits with two different diameters and two separate operations for each slot - which is time consuming, and is one of the weaknesses of the new joining technique. Nevertheless, the proposed solution is completely externally invisible. It does not require the use of glue. It is practical to use for cabinet furniture.

Recapitulating, it ought to be stressed that the designed and tested joint exhibited an increase in stiffness and strength together with the increase in the number of fasteners and their length. Longer fasteners were more easily mounted in slots and moved, and panel elements were more easily tightened upon them. After assembly, individual elements fit precisely, assured aesthetic appearance, and maintained the possibility of disassembly.

At last we should discuss a case in which no adhesive is used in the joints. Thanks the friction forces T and the assembly forces FA , such joints cannot easily fail when they are loaded laterally. In addition, the rear wall protects all horizontal elements against horizontal displacement. So, presented joints can be considered as an "easy-to-assemble/disassemble" connection.

CONCLUSIONS

The results of the performed experimental investigations and numerical calculations allow formulation of the following conclusions and observations:

1. The designed joint with a dual-conical fastener was characterized by high stiffness and strength. Stiffness and strength of this joint increased with the increase in the number of fasteners and their length.
2. Within the range of linear elasticity, stresses in fasteners may attain the level of 58% of ABS strength.
3. Low stress levels in panel elements guaranteed durable and safe utilization of the designed joints to manufacture cabinet furniture both from MDF and fiberboard panels.
4. Ease of assembly and disassembly of joints without tools, external invisibility, good aesthetics, high resistance, and stiffness can ensure high potentials of the presented solution in industrial and trade practice.

REFERENCES CITED

- Altinok, M., Tas, H. H., and Çimen, M. (2009). "Effects of combined usage of traditional glue joint methods in box construction on strength of furniture," *Materials and Design* 30(8), 3313-3317. DOI: 10.1016/j.matdes.2008.12.004
- Altun, S., Burdurlu, E., and Kiliç, M. (2010). "Effect of adhesive type on the mending moment capacity of miter frame corner joints," *BioResources* 5(3), 1473-1483. DOI: 10.15376/biores.5.3.1473-1483
- Atar, M., and Özçifçi, A. (2008). "The effects of screw and back panels on the strength of corner joints in case furniture," *Materials and Design* 29(2), 519-525. DOI: 10.1016/j.matdes.2007.01.015
- Atar, M., Özçifçi, A., Altinok, M., and Celikel, U. (2009). "Determination of diagonal compression and tension performances for case furniture corner joints constructed with wood biscuits," *Materials and Design* 30(3), 665-670. DOI: 10.1016/j.matdes.2008.05.023
- Atar, M., Keskin, H., Peker, H., Ustündağ, A., Togay, A., and Candan, Z. (2010). "Impacts of different joint angles and adhesives on diagonal tension performances of box-type furniture," *BioResources* 5(1), 343-355. DOI: 10.15376/biores.5.1.343-355
- Ching, S. W., and Yiren, W. (1994). "A study on bending moment resistance of particleboard corner joint in carcass furniture," *Forest Product Industries* 13(4), 600-610.
- Derikvand, M., and Eckelman, C.A. (2015). "Bending moment capacity of L-Shaped mitered frame joints constructed of MDF and particleboard," *BioResources* 10(3), 5677-5690. DOI: 10.15376/biores.10.3.5677-5690
- Eckelman, C. A. (2003). *Textbook of Product Engineering and Strength Design of Furniture*, Purdue University Press, West Lafayette, IN.
- Efe, H., and Kasal, A. (2000). "Tensile strength of corner joint on the stable case and disassembled furniture," *Gazi University Journal of Industrial Arts Education Faculty* 8, 61-74.

- EN 310 (1994). "Wood-based panels. Determination of modulus of elasticity in bending and of bending strength," European Committee for Standardization, Brussels, Belgium.
- EN 323 (1993). "Wood-based panels. Determination of density," European Committee for Standardization, Brussels, Belgium.
- EN 322 (1993). "Wood-based panels. Determination of moisture content," European Committee for Standardization, Brussels, Belgium.
- İmirzi, H. Ö., and Efe, H. (2013). "Analysis of strength of corner joints in cabinet type furniture by using finite element method," *Proceedings of the XXVIth International Conference Research for Furniture Industry*, Poznan, Poland, pp. 49-55.
- Kasal, A. (2008). "Effect of the number of screws and screw size on moment capacity of furniture corner joints in case construction," *Forest Products Journal* 58(6), 36-44.
- Kasal, A., Şener, S., Belgin, Ç. M., and Efe, H. (2006). "Bending strength of screwed corner joints with different materials," *Gazi University Journal of Science* 19(3), 155-161.
- Kasal, A., Erdi, Y. Z., Zhang, J., Efe, H., and Avci, E. (2008a). "Estimation equations for moment resistances of L-type screw corner joints in case goods furniture," *Forest Products Journal* 58(9), 21-27.
- Kasal, A., Zhang, J., Yüksel, M., and Erdil, Y. Z. (2008b). "Effects of screw sizes on load bearing capacity and stiffness of five-sided furniture cases constructed of particleboard and medium density fiberboard," *Forest Products Journal* 58(10), 25-32.
- Kureli, I., and Altinok, M. (2011). "Determination of mechanical performances of the portable fasteners used on case furniture joints," *African Journal of Agricultural Research* 6(21), 4893-4901. DOI: 10.5897/AJAR11.284
- Liu, W. Q., and Eckelman, C. A. (1998). "Effect of number of fasteners on the strength of corner joints for cases," *Forest Products Journal* 48(1), 93-95.
- Maleki, S., Haftkhani, A. R., Dalvand, M., Faezipour, M., and Tajvidi, M. (2012). "Bending moment resistance of corner joints constructed with spline under diagonal tension and compression," *Journal of Forestry Research* 23(3), 481-490. DOI: 10.1007/s11676-012-0288-7
- Malkoçoğlu, A., Yerlikaya, N. Ç., and Çakiroğlu, F. L. (2013). "Effects of number and distance between dowels of ready-to-assemble furniture on bending moment resistance of corner joints," *Wood Research* 58(4), 671-680.
- Nicholls, T., and Crisan, R. (2002). "Study of the stress-strain state in corner joints and box type furniture using finite element analysis (FEA)," *Holz als Roh-und Werkstoff* 60(1), 67-71. DOI: 10.1007/s00107-001-0262-0
- NT BUILD 316 (1986). "Particle boards: Modulus of elasticity in tension and tensile strength. Nordtest method."
- Örs, Y., and Efe, H. (1998). "The mechanical behavior properties of fasteners in furniture design for frame construction," *Turkish Journal of Agriculture and Forestry* 22, 21-28.
- Rajak, Z., and Eckelman, C.A. (1996). "Analysis of corner joints constructed with large screws," *Journal of Tropical Forest Products* 2(1), 80-92.
- Smardzewski, J. (2015a). "Złącze stożkowe i połączenie kątowe, zwłaszcza do mebli skrzyniowych," *Zgłoszenie patentowe w UP RP, Poland, number P.412167*.
- Smardzewski, J. (2015b). *Furniture Design*, Springer, Heidelberg, Germany. DOI: 10.1007/978-3-319-19533-9

- Smardzewski, J., İmirzi, H. Ö., Lange, J., and Podskarbi, M. (2015). "Assessment method of bench joints made of wood-based composites," *Composite Structures* 123, 123-131. DOI: 10.1016/j.compstruct.2014.12.039
- Tankut, A. N. (2005). "Optimum dowel spacing for corner joints in 32-mm cabinet construction," *Forest Products Journal* 55(12), 100-104.
- Tankut, A. N., and Tankut, N. (2008). "Investigations the effects of fastener, glue, and composite material types on the strength of corner joints in case-type furniture construction," *Materials and Design* 30(10), 4175-4182. DOI: 10.1016/j.matdes.2009.04.038
- Tankut, A. N., and Tankut, N. (2010). "Evaluation the effects of edge banding type and thickness on the strength of corner joints in case-type furniture," *Materials and Design* 31(6), 2956-2963. DOI: 10.1016/j.matdes.2009.12.022
- Vassiliou, V., and Barboutis, I. (2005). "Screw withdrawal capacity used in the eccentric joints of cabinet furniture connectors in particleboard and MDF," *Journal of Wood Science* 51(6), 572-576. DOI: 10.1007/s10086-005-0708-9
- Yerlikaya, N. Ç. (2012). "Effects of glass-fiber composite, dowel, and minifix fasteners on the failure load of corner joints in particleboard case-type furniture," *Materials and Design* 39, 63-71. DOI: 10.1016/j.matdes.2012.02.024
- Yerlikaya, N. Ç., and Aktas, A. (2012). "Enhancement of load-carrying capacity of corner joints in case-type furniture," *Materials and Design* 37, 393-401. DOI: 10.1016/j.matdes.2012.01.010
- Zhang, J. L., and Eckelman, C. A. (1993). "The bending moment resistance of single dowel corner joints in case construction," *Forest Products Journal* 43(6), 19-24.
- Zhang, J. L., Efe, H., Erdil, Y. Z., Kasal, A., and Han, N. (2005). "Moment resistance of multi-screw L-type corner joints," *Forest Products Journal* 55(10), 56-63. <http://www.materialise.pl> (available 30.11.2015).

Article submitted: October 3, 2015; Peer review completed: November 23, 2015; Revised version received and accepted: December 1, 2015; Published: December 14, 2015.
DOI: 10.15376/biores.11.1.1224-1239